HEPATOLOGY

HEPATOLOGY, VOL. 0, NO. 0, 2019

Tissue Repair in the Mouse Liver Following Acute Carbon Tetrachloride Depends on Injury-Induced Wnt/β-Catenin Signaling

Ludan Zhao,[1,2] Yinhua Jin,[1] Katie Donahue,[1] Margaret Tsui,[3] Matt Fish,[1] Catriona Y. Logan,[1] Bruce Wang,[1,3] and Roel Nusse[1]

In the liver, Wnt/β-catenin signaling is involved in regulating zonation and hepatocyte proliferation during homeostasis. We examined Wnt gene expression and signaling after injury, and we show by *in situ* hybridization that Wnts are activated by acute carbon tetrachloride (CCl_4) toxicity. Following injury, peri-injury hepatocytes become Wnt-responsive, expressing the Wnt target gene axis inhibition protein 2 (Axin2). Lineage tracing of peri-injury Axin2$^+$ hepatocytes shows that during recovery the injured parenchyma becomes repopulated and repaired by Axin2$^+$ descendants. Using single-cell RNA sequencing, we show that endothelial cells are the major source of Wnts following acute CCl_4 toxicity. Induced loss of β-catenin in peri-injury hepatocytes results in delayed repair and ultimately injury-induced lethality, while loss of Wnt production from endothelial cells leads to a delay in the proliferative response after injury. *Conclusion:* Our findings highlight the importance of the Wnt/β-catenin signaling pathway in restoring tissue integrity following acute liver toxicity and establish a role of endothelial cells as an important Wnt-producing regulator of liver tissue repair following localized liver injury. (Hepatology 2019;0:1-13).

As a major site for both nutrition and xenobiotic metabolism, the liver serves as a first line of defense against environmental toxins. However, the liver can also be easily damaged by the compounds which it metabolizes. As such, the ability to repair damaged liver tissue has garnered much interest. What is the source of hepatocytes after injury? And how is hepatocyte repopulation regulated during injury repair?

In the context of many injury models, mature hepatocytes become activated to generate hepatocytes during injury repair.[1,2] It has also been suggested that following certain forms of liver injury and/or under conditions where hepatocyte proliferation is impaired, bipotential progenitor cells arising in the periportal region are activated to give rise to both cholangiocytes and hepatocytes, thus serving as a source of cells in injury repair.[3-7] However, the source of these bipotential cells has been debated.[2,6] In either case, the proproliferative signals induced by injury to activate hepatocyte proliferation remain to be fully characterized.

The Wnt/β-catenin signaling pathway has been implicated in the regulation of liver biology from normal development to disease.[8-11] Previous work, including

Abbreviations: Adgre1, adhesion G protein–coupled receptor E1; Bcat-cKO, Axin2Cre^{ERT2}; β-catenin$^{flox/\Delta}$; CMV-Cre, cytomegalovirus–cyclization recombination; EdU, 5-ethynyl-2′-deoxyuridine; Glt1, glutamate transporter 1; GS, glutamine synthetase; H&E, hematoxylin and eosin; PBS, phosphate-buffered saline; Pecam1, platelet/endothelial cell adhesion molecule 1; PFA, paraformaldehyde; Reln, Reelin; scRNA-seq, single-cell RNA sequencing; Tbx3, T-box transcription factor 3; Wls-cKO, Cdh5(PAC)Cre^{ERT2}; Wls$^{flox/\Delta}$.

Received March 16, 2018; accepted January 28, 2019.

Additional Supporting Information may be found at onlinelibrary.wiley.com/doi/10.1002/hep.30563/suppinfo.

Supported in part by the National Institutes of Health (T32GM007365 to L.Z., and K08DK101603 to B.W.) and in part by the Burroughs Wellcome Fund Career Award for Medical Scientists (to B.W.). R.N. is an investigator of the Howard Hughes Medical Institute.

View this article online at wileyonlinelibrary.com.

DOI 10.1002/hep.30563

Potential conflict of interest: Dr. Nusse consults for and owns stock in Surrozen. He owns stock in Bio-Techne.

from our lab, has shown that endothelium-derived Wnt signaling regulates pericentral hepatocyte proliferation during homeostasis. We showed that Wnts secreted by central vein endothelial cells maintain pericentral axis inhibition protein 2 $(Axin2)^+$ hepatocytes in a proliferative state.[12] In the context of partial hepatectomy, it has been shown that β-catenin is necessary for early postinjury hepatocyte DNA synthesis.[13-15] This effect following partial hepatectomy is regulated by macrophage-derived[13] and endothelium-derived[16] Wnts and is further modulated by the Wnt coactivator R-spondin 3, which signals through the leucine-rich repeat–containing G protein–coupled receptor 5 (Lgr5) receptor.[17,18] However, the role of Wnt/β-catenin signaling following acute localized liver injury, such as that following CCl_4 toxicity, remains to be fully understood.

Given the importance of the Wnt/β-catenin pathway in regulating hepatocyte proliferation, we asked whether this pathway is involved in regulating proliferation following acute carbon tetrachloride (CCl_4) injury.

Materials and Methods

ANIMALS AND CCl_4 INJURY

All injury experiments were performed on male mice, 8-12 weeks of age. All animals received a single intraperitoneal injection of 1 mL/kg CCl_4 (Sigma; diluted 1 to 4 in corn oil and filtered using a 0.2-μm filter prior to administration), unless otherwise stated. Administration of 1 mL/kg filtered corn oil was used for all uninjured controls. All mice were in the C57/BL6 background unless otherwise specified. C57/BL6J wild-type mice from the Jackson Laboratory were used for all experiments unless otherwise specified. Axin2-LacZ[19] and $Axin2Cre^{ERT2}$[20] mice have been described. Ai9 (B6.Cg-*Gt(ROSA)26Sor*$^{tm9(CAG-tdTomato)Hze}$/J),[21] $\beta\text{-catenin}^{flox}$ (B6.129-*Ctnnb1*^{tm2Kem}/KnwJ),[22] Wls^{flox} (129S-*Wls*$^{tm1.1Lan}$/J),[23] and cytomegalovirus–cyclization recombination (CMV-Cre; B6.C-Tg[CMV-cre] 1Cgn/J)[24] mice were obtained from the Jackson Laboratory. $Cdh5(PAC)Cre^{ERT2}$[25] were obtained from R. Adams. All alleles were heterozygous, except where stated.

To generate mice harboring deletion alleles for β-catenin ($\beta\text{-catenin}^{\Delta}$) or Wntless ($Wls^{\Delta}$), homozygous $\beta\text{-catenin}^{flox/flox}$ (or $Wls^{flox/flox}$) mice were crossed to CMV-Cre mice. Genotyping PCR to detect the deletion allele was carried out as described.[22,23]

For postinjury lineage tracing studies, $Axin2Cre^{ERT2}$; Ai9 mice received a single intraperitoneal injection of tamoxifen (Sigma; 4 mg tamoxifen per 25 g body weight, dissolved in 10% ethanol/corn oil) 24 hours after CCl_4 administration (n = 3 animals per time point).

For β-catenin knockout studies, CCl_4-injured $Axin2Cre^{ERT2}$; $\beta\text{-catenin}^{flox/\Delta}$ (Bcat-cKO) and $\beta\text{-catenin}^{flox/\Delta}$ littermate control mice received daily intraperitoneal 4 mg/25 g tamoxifen injections for 3 or 4 days, starting on the day of injury. Mice were sacrificed at day 2 (control n = 3, Bcat-cKO n = 3) or day 4 (control n = 3, Bcat-cKO n = 5) after injury. For injury survival studies, Bcat-cKO animals that received 1 mL/kg corn oil and four daily doses of tamoxifen were used for uninjured Bcat-cKO controls.

ARTICLE INFORMATION:

From the [1]Institute for Stem Cell Biology and Regenerative Medicine, Department of Developmental Biology, Howard Hughes Medical Institute; [2]Medical Scientist Training Program, Stanford School of Medicine, Stanford, CA; [3]Department of Medicine and Liver Center, University of California San Francisco, San Francisco, CA.

ADDRESS CORRESPONDENCE AND REPRINT REQUESTS TO:

Roel Nusse, Ph.D.
Lorry Lokey Stem Cell Research Building
265 Campus Drive, Room G2143
Stanford, CA 94305
E-mail: rnusse@stanford.edu
Tel.: +1-650-723-7769
or

Bruce Wang, M.D.
Health Science East 1427
513 Parnassus Ave
San Francisco, CA 94143-1346
E-mail: bruce.wang@ucsf.edu
Tel.: +1-415-476-6160

For Wntless knockout studies, Cdh5(PAC)Cre^{ERT2}; Wls$^{flox/\Delta}$ (n = 3) and Cdh5(PAC)Cre^{ERT2}; Wls$^{+/flox}$ or Wls$^{+/flox}$ littermate control (n = 4) mice received a single intraperitoneal injection of 0.75 mL/kg CCl_4 and daily doses of 4 mg/25 g tamoxifen for 3 days. All animals also received an intraperitoneal dose of 50 mg/kg of 5-ethynyl-2′-deoxyuridine (EdU; Invitrogen) 3 hours prior to sacrifice.

All animal experiments and methods were approved by the Institutional Animal Care and Use Committee at Stanford University in accordance with National Institutes of Health guidelines. All mice were housed in recyclable, individually ventilated cages in the Stanford University animal facility on a 12-hour light/dark cycle with *ad libitum* access to water and normal chow. All interventions were done during the light cycle.

HISTOLOGY AND IMMUNOFLUORESCENCE

For liver morphology analysis, collected liver samples were fixed in 10% neutral buffered formalin overnight at room temperature, serially dehydrated in ethanol, cleared in HistoClear (Natural Diagnostics), and paraffin-embedded in Paraplast Plus (Sigma). Paraffin sections (5 μm) were stained with Mayer's hematoxylin and counterstained with eosin.

For detection of LacZ expression in Axin2-LacZ samples, whole livers were fixed in 1% paraformaldehyde (PFA) overnight at 4°C, washed in detergent rinse (phosphate-buffered saline [PBS] with 2 mM $MgCl_2$, 0.01% sodium deoxycholate, and 0.02% Nonidet P40 [NP-40]), and stained in X-gal staining solution (PBS with 2 mM $MgCl_2$, 0.01% sodium deoxycholate, 0.02% NP-40, 5 mM potassium ferricyanide, and 1 mg/mL 5-bromo-4-chloro-3-indolyl-β-D-galactopyranoside) in the dark at room temperature for 4 days for full tissue penetration. Following staining, tissues were washed, postfixed in 4% PFA for 1 hour at room temperature, and processed for paraffin embedding.

For immunofluorescence antibody staining, samples were fixed in 4% PFA overnight at 4°C, cryoprotected in 30% sucrose in PBS for 24 hours at 4°C, embedded in optimal cutting temperature compound, and snap-frozen. Cryosections (8-10 μm) were blocked in 5% normal donkey serum in 0.5% Triton-X in PBS at room temperature and stained with primary and secondary antibodies, then mounted in Prolong Gold with 4′,6-diamidino-2-phenylindole mounting medium (Life Technologies). The Mouse on Mouse detection kit (Vector Labs) was used for all mouse primary antibody staining. The following primary antibodies were used: glutamine synthetase (GS; mouse, 1:500; Millipore MAB302), glutamate transporter 1 (Glt1; rabbit, 1:100; Frontier Institute Glt1-Rb-Af670), hepatocyte nuclear factor 4a (mouse, 1:100; Abcam ab41898), beta-actin (rabbit, 1:250; Abcam ab8227), T-box transcription factor 3 (Tbx3; goat, 1:50; Santa Cruz sc-17871), and Alexa Fluor 488 phalloidin (Thermo Fischer A12379). EdU detection was performed according to the Click-iT EdU Alexa Fluor 647 Imaging Kit (Life Technologies) protocol. All immunofluorescence staining was performed in the dark.

RNA ISOLATION AND REAL-TIME QUANTITATIVE PCR

Liver samples were homogenized in TRIzol (Invitrogen) using a benchtop bead homogenizer, and RNA isolation was carried out per product protocol. Isolated RNA was purified using the RNeasy Mini Isolation Kit (Qiagen) per product protocol. RNA reverse transcription was performed using the High Capacity Reverse Transcription Kit (Life Technologies), and real-time quantitative PCR was performed using duplex Taqman Gene Expression Assays (Axin2, Wnt2, Wnt4, Wnt5a, Wnt9b, albumin, Ki67, and glyceraldehyde 3-phosphate dehydrogenase; Life Technologies), run in 96-well plate format on the StepOnePlus Real-Time PCR System (Applied Biosystems). No-template controls were also performed. Relative target gene expression levels were calculated using the delta-delta CT method.[26] The gene expression level of the mutant was normalized to that of the control. Statistical significance in relative expression levels was analyzed with one-way analysis of variance in GraphPad Prism 7.

RNA SCOPE *IN SITU*

Paraffin-embedded liver sections were processed for RNA *in situ* detection using either the RNAscope 1-plex Detection Kit (Chromogenic) for single *in situ* experiments or the RNAScope 2.5 HD Duplex Kit for double *in situ* experiments, according

to the manufacturer's protocol (Advanced Cell Diagnostics). The following RNAscope probes were used: Axin2 (NM 015732, region 330-1287), Wnt2 (NM 023653, region 857-2086), Wnt4 (NM 009523.2, region 2147-3150), Wnt5a (NM 009524.3, region 200-1431), Wnt9b (NM 011719, region 727-1616), platelet/endothelial cell adhesion molecule 1 (Pecam1; NM 001032378.1, region 915-1827), adhesion G protein–coupled receptor E1 (Adgre1; NM 010130.4, region 85-1026), Reelin (Reln; NM 011261.2, region 9371-10257), 4-hydroxy-tetrahydrodipicolinate reductase (negative control, EF 191515, region 414-862), and RNA polymerase II subunit a (positive control, NM 009089.2, region 2802-3678).

SINGLE-CELL RNA SEQUENCING

Single-cell suspensions were generated from day 3 CCl_4-injured mice by a modified two-step collagenase perfusion technique, as described.[12] Hepatocytes were removed by low-speed centrifugation. Nonparenchymal cells were captured as single cells and sequenced with the 10× Genomics droplet-based method.[27] CellRanger version 2.1.1 was used to align raw reads and to filter cell barcodes. Quality control, principal component analysis, clustering, and differential expression analysis were performed in R with the Seurat version 2.3.4 package.[27] Samples with disproportionally high cell counts were randomly down-sampled to the group average. Cells with fewer than 200 or greater than 3,000 genes, a unique molecular identifier count of fewer than 500 or greater than 10,000, and >25% of total expression from mitochondrial genes were filtered out. An initial round of clustering was performed to identify and remove hepatocytes. The remaining cells were subclustered and annotated using markers for known nonparenchymal cell types in the liver (Supporting Fig. S6D).

MICROSCOPY AND IMAGING

All immunohistochemistry, RNA *in situ*, and immunostaining sections were imaged using a Zeiss Axioplan 2 microscope equipped with AxioCam MRm (fluorescence) and MRC5 (bright field) cameras. Image acquisition was done using Axiovision AC software (release 4.8; Carl Zeiss).

IMAGE QUANTIFICATION

For lineage tracing studies, thresholding was applied to single-channel fluorescent images, and the pixel area of the thresholded region was measured using ImageJ. "Percent labeled area" was calculated as percent total tdTomato-positive pixel area over total intact tissue area. For day 3 samples, total intact tissue area was defined as total tissue area minus necrotic tissue area. Ten or more representative images were analyzed per animal per time point.

For Bcat-cKO tissue repair analysis, hematoxylin and eosin (H&E) images were used for quantification. "Percent lobular repair" was defined as 1 – (injury distance/hepatic lobule distance) × 100%. Hepatic lobule distance was measured as the distance from the central vein to the portal vein. Injury distance was measured as the distance from the central vein to the injury border. A minimum of 10 hepatic lobules were analyzed per animal per timepoint.

Statistical analysis was conducted using a two-tailed *t* test on GraphPad Prism 7. All graphs were generated in GraphPad Prism 7.

Results

INJURY INDUCES *DE NOVO* Wnt RESPONSE IN MIDLOBULAR HEPATOCYTES

Previously, we had found that in the uninjured liver pericentral, Wnt-regulated Axin2$^+$ hepatocytes proliferate at a higher rate compared to other cells.[12] In our current studies, we asked whether Wnt/β-catenin signaling performs a similar role in regulating hepatocyte proliferation following acute liver injury. CCl_4 injury leads to centrilobular necrosis within 48 hours of CCl_4 administration (Supporting Fig. S1). The local effect of CCl_4 is due to the zonated expression of CYP2E1, the major P450 cytochrome that metabolizes CCl_4.[28] In order to determine whether Wnt signaling is activated following acute CCl_4 injury, we conducted *in situ* hybridization for the Wnt target gene, Axin2.[19,29] While expression of Axin2 is normally restricted to pericentral hepatocytes (Fig. 1A), its expression became undetectable as early as 6 hours following CCl_4 administration (Fig. 1B). However, Axin2 expression reappears in the injured liver by

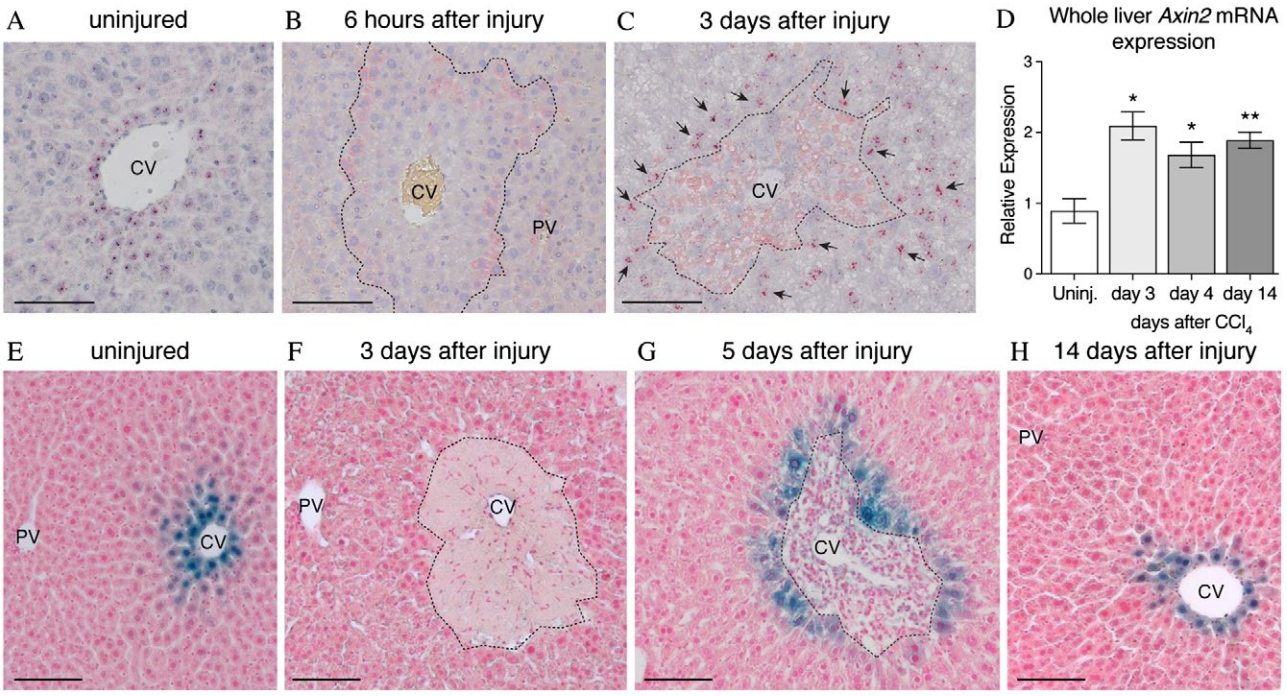

FIG. 1. CCl_4 injury induces *de novo* Axin2 expression in peri-injury hepatocytes. (A-C) Axin2 mRNA *in situ* hybridization in uninjured (A), early injured, and repairing livers shows that Axin2 expression is lost as soon as 6 hours after injury (B) but is reactivated in peri-injury hepatocytes during injury repair (C, arrows). (D) Up-regulation of Axin2 expression following injury is confirmed by whole-liver quantitative RT-PCR. (E-H) Axin2-LacZ reporter staining also confirms the dynamics of *de novo* Axin2 expression in peri-injury hepatocytes following CCl_4 toxicity. Scale bars, 100 μm. Dashed line represents injury border. Error bars show SEM. $^*P < 0.05$, $^{**}P < 0.01$ by two-tailed *t* test compared to uninjured control for n = 3 animals per time point. Abbreviations: CV, central vein; PV, portal vein.

3 days following injury, but its expression is observed in *midlobular* hepatocytes as opposed to pericentral hepatocytes (Fig. 1C). Additionally, these injury-induced $Axin2^+$ hepatocytes encircle the local necrotic tissue, extending from directly adjacent to the injury border to a few cell diameters away (Fig. 1C, arrows). This postinjury up-regulation of Axin2 expression is consistent with whole-liver quantitative RT-PCR results which show significant up-regulation of Axin2 expression at 3 days after injury (Fig. 1D). Injury-induced expression of Axin2 is sustained throughout the injury repair time course (Fig. 1D), indicating that Wnt signaling is active during the entirety of injury repair.

Consistent with our *in situ* hybridization results, Axin2-LacZ reporter animals showed that while the original population of pericentral $Axin2^+$ hepatocytes (Fig. 1E) is lost following CCl_4 administration (Fig. 1F), surviving midlobular hepatocytes adjacent to the injury border begin to express Axin2 during injury repair (Fig. 1G). Interestingly, this pattern of injury-induced Axin2 expression in hepatocytes bordering the damaged tissue is maintained throughout tissue repair (Supporting Fig. S2). Upon full injury recovery, the normal homeostatic pattern of Axin2 expression, restricted to the pericentral cells, is reestablished (Fig. 1H). Thus, CCl_4 injury induces activation of a Wnt signaling response in surviving hepatocytes immediately adjacent to the damaged centrilobular region.

In the uninjured liver, pericentral $Axin2^+$ hepatocytes express both GS and Glt1 (Fig. 2A,E). Upon pericentral hepatocyte ablation following injury, GS and Glt1 are no longer expressed by the surviving hepatocytes in the liver lobule (Fig. 2B,F). Over the course of injury repair, while rare peri-injury hepatocytes exhibit expression of GS (Fig. 2C, arrowhead), Glt1 expression remains negative (Fig. 2G). Finally, upon full injury recovery at 14 days following CCl_4, the homeostatic GS and Glt1 expression patterns are reestablished in pericentral hepatocytes (Fig. 2D,H).

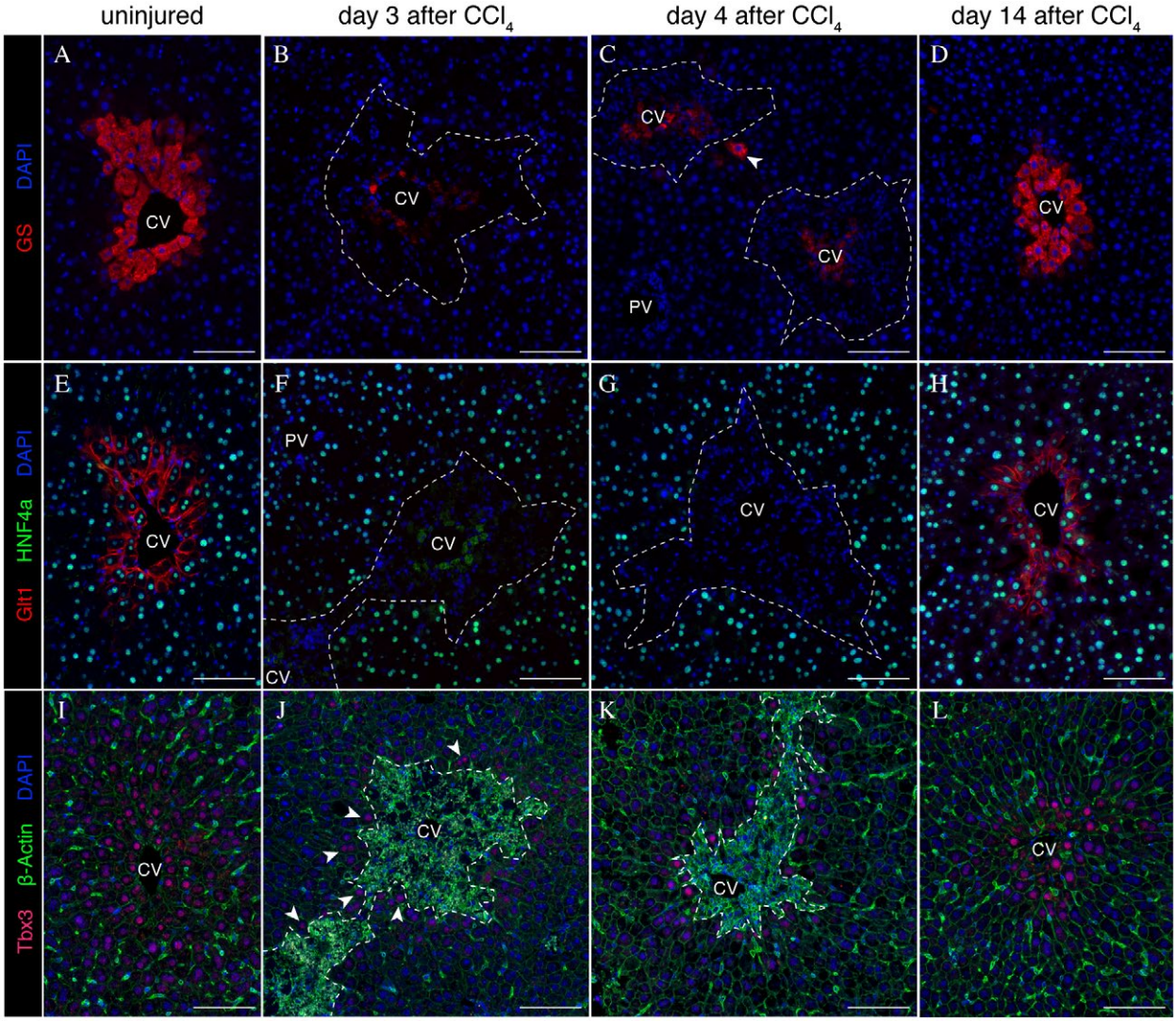

FIG. 2. Post-CCl_4 peri-injury hepatocytes do not express Wnt targets GS and Glt1 but are positive for Tbx3. (A-D) Expression of GS in uninjured (A) and postinjury (B-D) liver. Rare GS^+ hepatocytes are observed during injury repair (C, arrowhead). (E-H) Expression of Glt1 in uninjured (E) and postinjury (B-D) liver. (I-L) Expression of Tbx3 in uninjured (I) and postinjury (J-L) liver. Low levels of Tbx3 expression are induced in peri-injury hepatocytes as early as 3 days following injury (J, arrowheads). Scale bars, 100 μm. Dashed line represents injury border. Representative images from n = 3 animals per time point. Abbreviations: CV, central vein; DAPI, 4′,6-diamidino-2-phenylindole; HNF4a, hepatocyte nuclear factor 4a; PV, portal vein.

These results provide evidence that injury-induced $Axin2^+$ hepatocytes, which are located in the mid-hepatic lobule, adjacent to the injury border, do not express GS or Glt1 and are thus distinct from pericentral $Axin2^+$ cells of the uninjured liver.

Previously, we reported that pericentral $Axin2^+$ hepatocytes in the uninjured adult liver express the early hepatocyte marker Tbx3[12] (Fig. 2I). Strikingly, while pericentral $Tbx3^+$ hepatocytes are lost following injury, Tbx3 expression is turned on in peri-injury hepatocytes throughout the injury repair process (Fig. 2J,K). By 14 days following injury, the pericentral Tbx3 expression pattern is reestablished (Fig. 2L).

PERI-INJURY AXIN2$^+$ HEPATOCYTES PROLIFERATE TO REPAIR LOCAL INJURY

To determine whether injury-induced peri-injury $Axin2^+$ hepatocytes proliferate in response to injury,

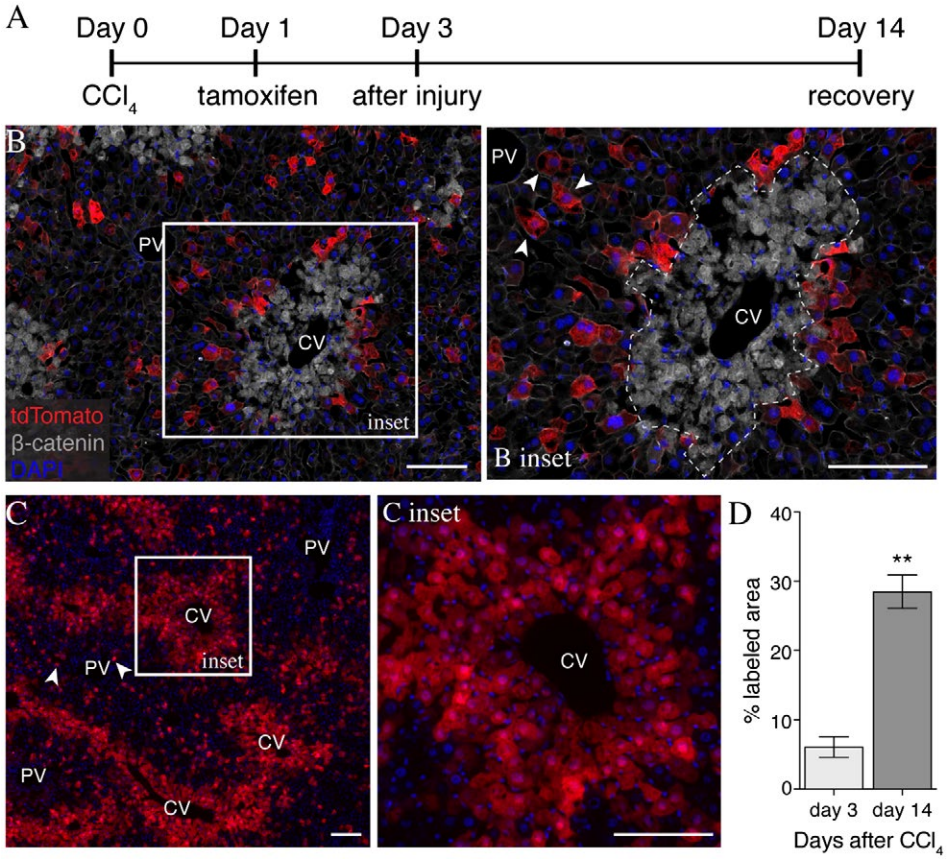

FIG. 3. Peri-injury Axin2$^+$ hepatocytes proliferate to repair damaged tissue. (A) Injury and lineage labeling scheme for (B-D). Peri-injury Axin2$^+$ hepatocytes are efficiently labeled following injury (B) and show significant expansion over the course of tissue repair (C). Notably, tdTomato$^+$ hepatocytes in the periportal space (B inset, arrowheads) show no expansion upon injury repair (C, arrowheads). (D) Quantification of percent labeled area. Scale bars, 100 μm. Dashed line represents injury border. Error bars show SEM. $^{**}P < 0.01$ by two-tailed *t* test for n = 3 animals per time point. Abbreviations: CV, central vein; PV, portal vein.

we performed lineage tracing of Axin2$^+$ hepatocytes, using tamoxifen-inducible Axin2Cre^{ERT2}; Ai9 reporter mice, after CCl_4 injury (Fig. 3A). At 3 days following injury, peri-injury Axin2$^+$ hepatocytes were labeled with cytoplasmic tdTomato (6.0 ± 2.6% of total area; Fig. 3B,D). Upon full recovery at 14 days after injury, labeled hepatocytes and their progeny accounted for 28.4 ± 4.2% of the total liver tissue (Fig. 3D). Significantly, all central veins at 14 days after injury were lined with rings of labeled hepatocytes (Fig. 3C, inset), indicating that peri-injury Axin2$^+$ hepatocytes are the main source of repopulation of the damaged centrilobular tissue.

We also found that some periportal hepatocytes were labeled following injury (Fig. 3B inset, arrowheads). However, these labeled periportal cells did not expand into clones upon injury recovery (Fig. 3C, arrowheads). The lack of clone generation by labeled periportal hepatocytes suggests that it is peri-injury hepatocytes, and not hepatocytes elsewhere in the hepatic lobule, that are activated to proliferate following injury.

UP-REGULATION OF ENDOGENOUS AND EXOGENOUS Wnt LIGANDS FOLLOWING INJURY

In the uninjured liver, Wnt2 and Wnt9b are expressed in the endothelial cells lining the central vein,[12] while Wnt2 is also expressed in sinusoidal endothelial cells.[12,16,30] We conducted a quantitative RT-PCR Wnt screen at various time points following injury to identify those Wnts whose expression may

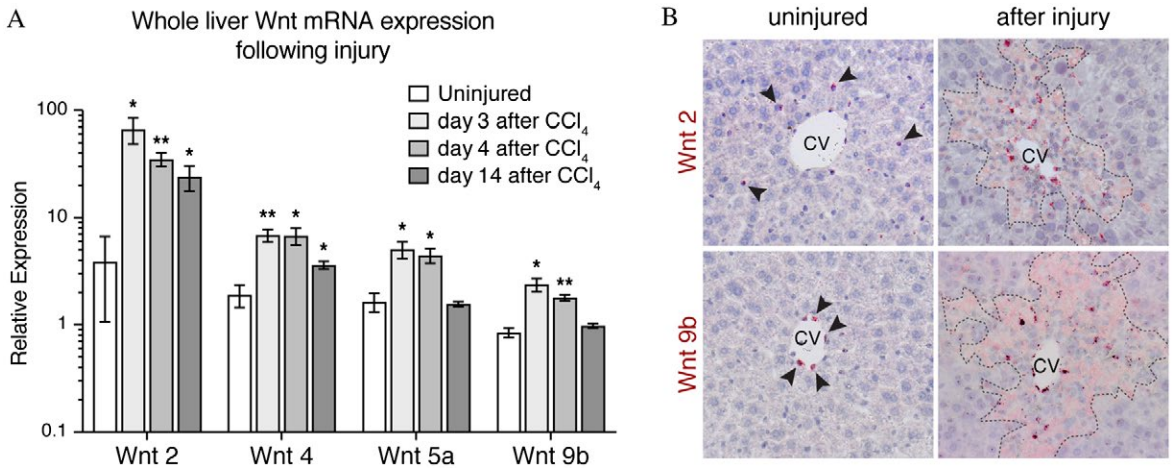

FIG. 4. Up-regulation and expression pattern of Wnt ligands after injury. (A) Whole-liver quantitative RT-PCR results showed significant ($P < 0.05$) up-regulation of four Wnt ligands whose expression is found in the pericentral and midlobular regions following injury. (B) mRNA *in situ* hybridization for Wnt2 and Wnt9b show expanded regions of expression for these two pericentral Wnt ligands early after injury. Arrowheads indicate positive signal in the uninjured liver. *In situ* hybridization images for Wnt4 and Wnt5a can be found in Supporting Fig. S5. Dashed lines represent injury border. Error bars show SEM. $^{*}P < 0.05$, $^{**}P < 0.01$ by two-tailed *t* test for n = 3 animals per time point. Abbreviation: CV, central vein.

be up-regulated following CCl_4 injury. We found that Wnt2, Wnt4, Wnt5a, and Wnt9b were significantly up-regulated following injury and throughout injury repair (Fig. 4A). *In situ* hybridization studies on injured liver sections confirmed the expression of these four Wnt ligands within and/or around the necrotic lesion (Fig. 4B; Supporting Fig. S5). While the expression of Wnt2 and Wnt4 persisted at higher levels following injury repair 2 weeks after CCl_4 administration, the expression of Wnt5a and Wnt9b returned to normal levels by 14 days after injury (Fig. 4A; Supporting Fig. S5).

The liver-endogenous Wnt2 and Wnt9b were found to be expressed in the locally damaged tissue during both the early necrotic phase (Supporting Fig. S5) as well as the active repair phase (Fig. 4B) following CCl_4 administration. By *in situ* hybridization, the expression pattern of these two Wnts appeared to radiate outward from the central vein endothelial cells and into the locally damaged tissue but not beyond the injury border. Of note, the expression pattern of Wnt9b, normally restricted to central vein endothelial cells, is significantly broadened following injury (Fig. 4B). The observation that Wnt2 and Wnt9b expression persists throughout the injury and repair phases after CCl_4 combined with the proximity of these Wnts to the injury border makes these Wnts likely candidates as the ligands which activate the postinjury Wnt response in peri-injury $Axin2^{+}$ hepatocytes.

ENDOTHELIAL CELLS ARE THE MAJOR SOURCE OF Wnts AFTER INJURY

Our *in situ* hybridization studies (Supporting Fig. S5) suggested that nonparenchymal cells were the major source of Wnt ligands following injury. To further identify the cellular source of Wnt ligands after acute CCl_4 injury, we conducted single-cell RNA sequencing (scRNA-seq) on liver nonparenchymal cells in day 3 CCl_4-injured mouse livers. T-distributed stochastic neighbor embedding analysis identified seven clusters of nonparenchymal cells in the injured liver (Fig. 5A). Our analysis showed that upon injury Wnt2 and Wnt9b are highly expressed in endothelial cells, while Wnt4 is expressed in stellate cells (Fig. 5B). Very few Wnt5a-expressing cells were captured in our scRNA-seq experiments (Supporting Fig. S6F).

To localize the Wnt-producing cells in the injured liver lobule, we conducted double *in situ* hybridization for Wnt2, Wnt4, Wnt5a, and Wnt9b and specific

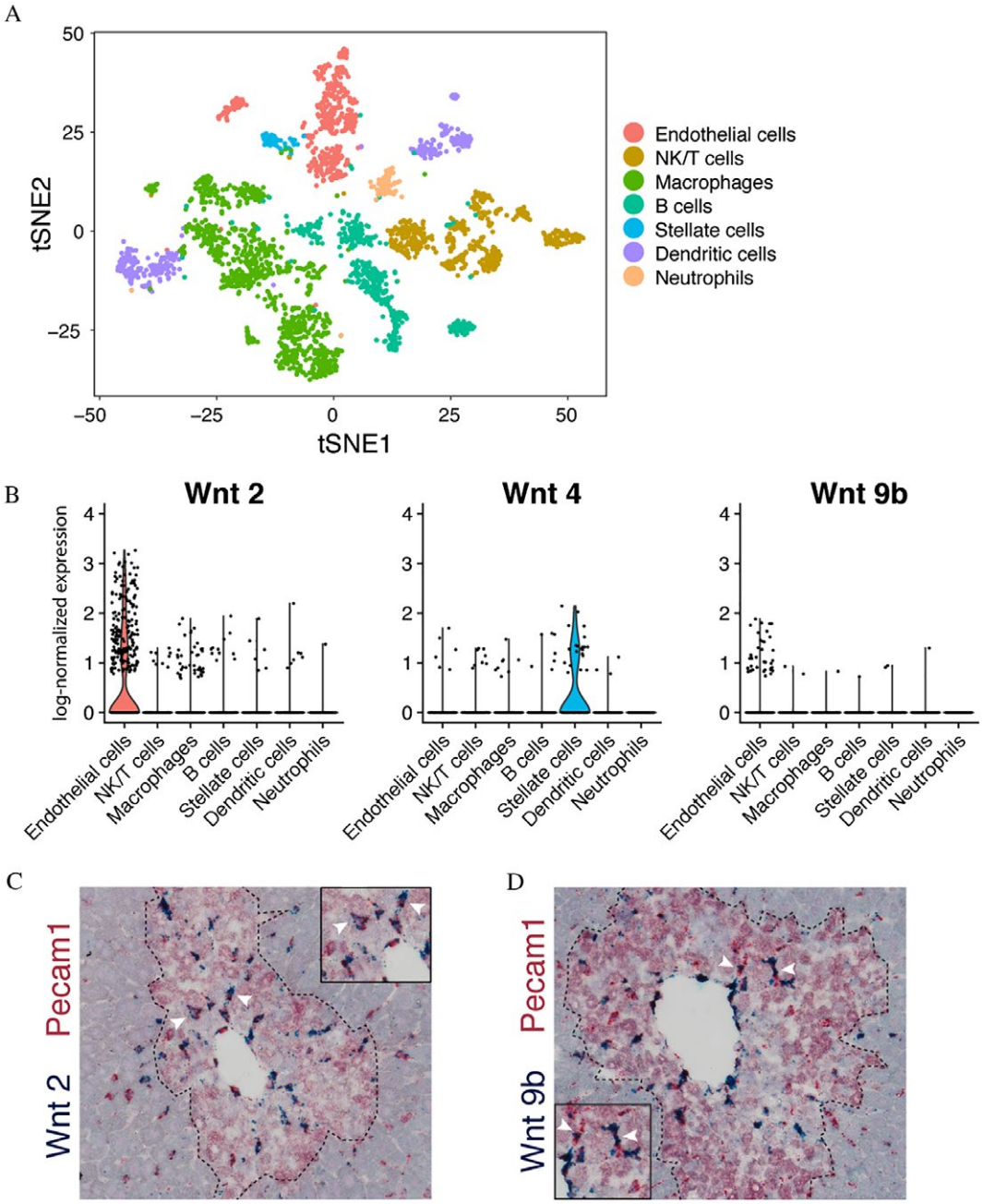

FIG. 5. Endothelial cells are the major source of Wnt2 and Wnt9b after injury. (A) T-distributed stochastic neighbor embedding plot showing seven clusters of nonparenchymal cells in the day 3 CCl_4-injured (n = 3,115 cells) livers. Colors denote different cell types as shown in the legend. Markers used to identify specific cell types are shown in Supporting Fig. S6D. (B) Violin plots of log-normalized expression (natural logarithm of 1+ counts per 10,000) of Wnt2, Wnt4, and Wnt9b in the injured liver, categorized by cell type. Double *in situ* hybridization of Pecam1 (red) and (C) Wnt2 (blue) and (D) Wnt9b (blue) shows significant overlap between Pecam1 and these two Wnts. Arrowheads denote examples of double-positive cells. Dashed line denotes injury border. n = 3 animals for all studies shown. Abbreviations: NK, natural killer; tSNE, T-distributed stochastic neighbor embedding.

cell markers for endothelial cells (Pecam1), Kupffer cells (Adgre1), and stellate cells (Reln) (Supporting Fig. S7). Consistent with the scRNA-seq results, double *in situ* hybridization revealed that in the injured liver Wnt2 and Wnt9b expression strongly overlapped with Pecam1 expression (Fig. 5C,D) but

not with Adgre1 or Reln expression (Supporting Fig. S7). A subset of Wnt4-expressing cells and a subset of Wnt5a-expressing cells also expressed Reln; however, neither of these two Wnts showed significant overlap with Pecam1 or Adgre1 expression (Supporting Fig. S6). Thus, after injury, endothelial cells are the major source of Wnt2 and Wnt9b, while stellate cells specifically express Wnt4.

Wnt SIGNALING IS REQUIRED FOR INJURY REPAIR

To test whether injury-induced Wnt signaling is required for tissue repair following acute CCl_4, we interfered with the intracellular Wnt signaling response by conditionally knocking out β-catenin in Wnt-responding cells in Bcat-cKO mice after CCl_4 administration. Following tamoxifen-induced β-catenin knockout, Axin2 expression was significantly down-regulated in Bcat-cKO animals after injury compared to controls (Fig. 6A). Furthermore, *in situ* hybridization showed that Axin2 mRNA was specifically down-regulated in peri-injury hepatocytes (Fig. 6B), indicating that loss of β-catenin in $Axin2^+$ cells effectively dampened the Wnt response in these cells. H&E staining revealed that while both control and Bcat-cKO animals exhibited similar initial injury response to 1 mL/kg CCl_4 (Supporting Fig. S9), Bcat-cKO livers appeared significantly more damaged when compared to control livers by 4 days following injury (Fig. 6C,D). This result suggests that loss of Wnt response in peri-injury hepatocytes led to a delay in the repopulation of the damaged lesion.

To determine whether this initial delay in injury repair persists throughout the injury repair process, we conducted experiments to assess the rate of repair at later time points following CCl_4 administration. However, we found instead that injured Bcat-cKO animals showed a higher rate of injury-induced lethality. While three out of five injured control animals survived at least 2 weeks after CCl_4 injury, Bcat-cKO animals had a median survival of 5 days after injury (Fig. 6E). It is known that loss of β-catenin from $Axin2^+$ cells also negatively affects intestinal homeostasis, and thus it is possible that the early lethality observed in injured Bcat-cKO animals could be attributable to extrahepatic effects such as that in the intestines. However, uninjured Bcat-cKO animals had a median survival of 10 days following β-catenin knockout, significantly higher than the median survival of injured Bcat-cKO animals (Fig. 6E). Together these data suggest that loss of the Wnt response in peri-injury hepatocytes following acute CCl_4 injury results in a delay in the repair of damaged tissue, which ultimately leads to lethality from CCl_4 toxicity.

To test further the necessity of Wnt signaling in injury repair, we examined whether endothelium-secreted Wnt ligands are critical by conditionally deleting Wntless (Wls) in $Cdh5(PAC)Cre^{ERT2}$; $Wls^{flox/\Delta}$ (Wls-cKO) mice. This knockout approach was effective at blocking injury-induced Wnt activation, as shown by decreased Axin2 expression in Wls-cKO livers compared to control livers (Fig. 6F). We also found that coincident with decreased Axin2 expression, Wls-cKO animals exhibited decreased Ki67 expression levels when compared to control animals (Fig. 6F). This result suggests that injury-induced cell proliferation is decreased upon loss of endothelial Wls. Consistent with the decreased Ki67 expression, hepatocyte incorporation of the thymidine-analogue EdU was also lower at day 3 following injury in Wls-cKO animals compared to controls (Fig. 6G; 4.1 ± 1.8% Wls-cKO versus 18.6 ± 7.4% control). However, neither injured control nor injured Wls-cKO animals survived past day 3 after injury, likely due to increased sensitivity to CCl_4 given the mixed background strain of these animals.[31] Thus, while hypersensitivity to CCl_4 in these mice prevented analysis at later injury time points, we did observe down-regulation of Ki67 and decreased hepatocyte EdU incorporation in Wls-cKO animals early after injury. These data suggest that block of endothelial Wnt secretion results in an overall decrease in the proliferative response of hepatocytes following injury and that postinjury endothelium-derived Wnt signaling is necessary for injury-induced hepatocyte proliferation.

Discussion

Adult tissue-specific stem cells maintain organ homeostasis and are activated following injury to mediate tissue repair.[32,33] However, how does tissue repair proceed upon targeted ablation of tissue-specific stem cells? In the intestines, $Lgr5^+$ intestinal epithelial cells form a population of mitotically active intestinal stem cells that maintain intestinal homeostasis.[34] However, upon ablation of these highly proliferative

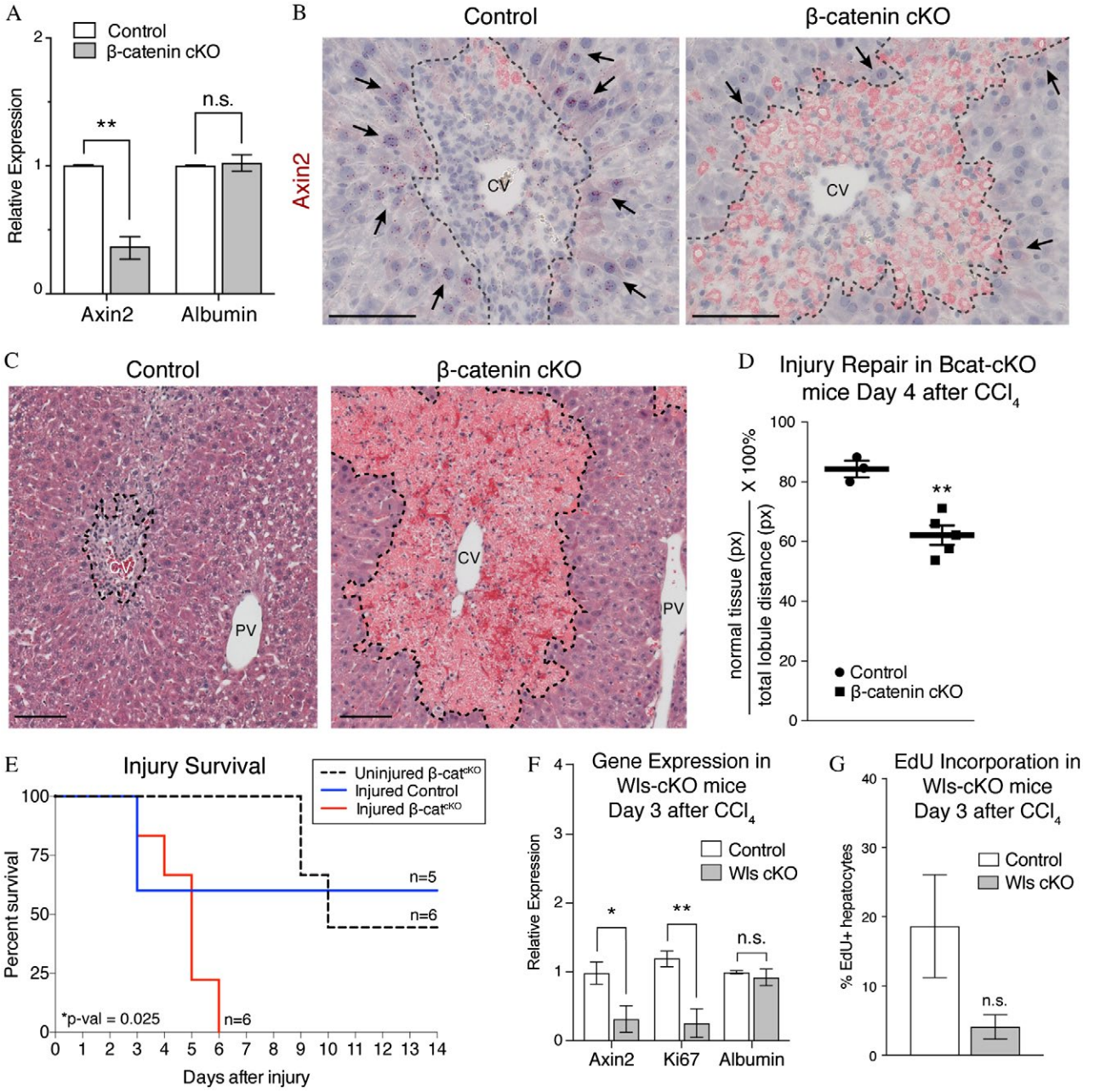

FIG. 6. Wnt/β-catenin signaling is necessary for injury repair and survival. (A) Inducible knockout of β-catenin in the CCl_4-injured liver results in a significant decrease in Axin2 expression as measured by whole-liver quantitative RT-PCR. (B) Axin2 expression is specifically down-regulated in peri-injury hepatocytes (arrows) upon loss of β-catenin in injured Bcat-cKO mouse livers (n = 3 control mice, n = 5 Bcat-cKO mice). (C) H&E staining morphology of injured control and Bcat-cKO livers at 4 days after injury. (D) Quantification of the extent of parenchymal repopulation based on image analysis of H&E-stained sections of injured livers (see Materials and Methods) shows that injured Bcat-cKO livers are significantly less repaired at 4 days following injury compared to injured control livers. (E) Loss of β-catenin ultimately results in lethality following CCl_4 injury. (F) Loss of Wntless in endothelial cells results in decreased Axin2 and Ki67 expression by whole-liver quantitative RT-PCR at 3 days after injury. (G) A concurrent decrease in hepatocyte EdU incorporation is also observed in Wls-cKO animals (n = 4 control mice, n = 3 Wls-cKO mice). Error bars show SEM. *$P < 0.05$, **$P < 0.01$ by two-tailed t test. Scale bars, 100 μm. Dashed line represents injury border. Abbreviations: CV, central vein; n.s., not significant; PV, portal vein.

stem cells by irradiation, a population of otherwise quiescent Bmi1-expressing cells facilitate repair and reepithelialization.[35] Thus, in the intestines, there exists a distinct "back-up" reservoir of cells that can contribute to tissue repair when the stem cell population active during homeostasis is lost.

We have previously shown that pericentral Axin2$^+$ hepatocytes contribute to normal liver homeostasis in the uninjured mouse liver.[12] Here, using the acute CCl_4 liver injury model, we efficiently eliminated these pericentral Axin2$^+$ hepatocytes. We found that injury results in increased expression in an expanded region of endogenous Wnt2 and Wnt9b. This injury-induced Wnt signaling activation results in a *de novo* Wnt response, in the form of Axin2 expression, in midlobular hepatocytes bordering the damaged local tissue. Peri-injury Axin2 expression is maintained throughout the repair time course, and sustained active Wnt signaling occurs at the dynamic boundary between damaged and undamaged liver tissue after injury. Our findings show that when the homeostatic source of hepatocytes is eliminated by CCl_4 injury, another population of Wnt-activated peri-injury hepatocytes can serve as the source of hepatocytes for repair.

Acute CCl_4 injury led to increased expression of Wnt2 and Wnt9b, the same Wnts that are normally expressed by centrilobular endothelial cells in the uninjured liver.[12,36] We took an unbiased scRNA-seq approach to identify the cellular sources of Wnts after injury and found that endothelial cells are the primary source of Wnt2 and Wnt9b following injury. These scRNA-seq results were supported by double *in situ* experiments which showed significant overlap in the expression of these Wnts with Pecam1 expression in sinusoidal endothelial cells. Our functional studies also showed that *in vivo* blockade of endothelial Wnt secretion resulted in a dampening of the proliferative response following injury. Together, our findings are in line with previous reports that have highlighted the importance of endothelial cells as a paracrine signaling center for regulating hepatocyte proliferation following injury.[16,30,37-39] Activation of the stroma-derived factor 1 receptor chemokine (C-X-C motif) receptor 7 on liver sinusoidal endothelial cells promotes a proregenerative environment by inducing hepatocyte growth factor and Wnt2 production following injury.[30] On the other hand, activation of the endothelial shear-stress inducible transcription factor Krüppel-like factor 2 upon injury inhibits hepatocyte proliferation, in part by promoting activin A production.[38] Therefore, paracrine signaling derived from liver endothelial cells serves as a check-and-balance system in regulating injury-induced hepatocyte proliferation.

Strikingly, we found that loss of the peri-injury hepatocyte Wnt response ultimately leads to failure to recover from CCl_4 injury. This result is in contrast to what has been observed in the context of partial hepatectomy, where knockout of β-catenin in hepatocytes led to an initial delay in hepatocyte entry into S phase but did not ultimately result in significant changes in liver mass recovery or survival after hepatectomy.[14,40]

Our findings show that following a *localized* injury (i.e., CCl_4), only select hepatocytes, specifically those closest to the damaged tissue, are more likely to become activated and undergo proliferation, while hepatocytes farther from the injury site remain quiescent. This is in contrast to the pan-hepatocyte proliferative response observed after a global liver injury such as partial hepatectomy. Additionally, our results show that most hepatocytes have the *capacity* to respond to a Wnt signal. This inherent capacity for hepatocellular response to Wnt signaling is biologically significant given the liver's increased risk for injury as a central detoxification organ and the major role of Wnt/β-catenin signaling as a regulator for liver tissue repair.

Acknowledgment: We thank T. Desai, J. Sage, L. Xing, S. Tan, H. Takase, J. Tsai, T. Anbarchian, E. Rim, E. Rulifson, W.C. Peng, and K. Loh for helpful discussions on experimental design and data analysis; G. Karnam, D. Burhan, and the University of California San Francisco Liver Center for assistance with liver cell isolations; P. Lovelace for assistance with flow cytometry; and K. Shaw for assistance in reagent and supplies acquisition.

REFERENCES

1) Malato Y, Naqvi S, Schürmann N, Ng R, Wang B, Zape J, et al. Fate tracing of mature hepatocytes in mouse liver homeostasis and regeneration. J Clin Invest 2011;121:4850-4860.
2) Yanger K, Knigin D, Zong Y, Maggs L, Gu G, Akiyama H, et al. Adult hepatocytes are generated by self-duplication rather than stem cell differentiation. Stem Cell 2014;15:340-349.
3) Newsome PN, Hussain MA, Theise ND. Hepatic oval cells: helping redefine a paradigm in stem cell biology. Curr Top Dev Biol 2004;61:1-28.
4) **Huch M**, **Dorrell C**, Boj SF, Van Es JH, Li VSW, van de Wetering M, et al. *In vitro* expansion of single Lgr5$^+$ liver stem cells induced by Wnt-driven regeneration. Nature 2013;494:247-250.

5) Tanimizu N, Mitaka T. Re-evaluation of liver stem/progenitor cells. Organogenesis 2014;10:208-215.
6) Tarlow BD, Finegold MJ, Grompe M. Clonal tracing of Sox9$^+$ liver progenitors in mouse oval cell injury. Hepatology 2014;60:278-289.
7) **Raven A**, **Lu W-Y**, Man TY, Ferreira-Gonzalez S, O'Duibhir E, Dwyer BJ, et al. Cholangiocytes act as facultative liver stem cells during impaired hepatocyte regeneration. Nature 2017;547:350-354.
8) Micsenyi A, Tan X, Sneddon T, Luo J-H, Michalopoulos GK, Monga SPS. Beta-catenin is temporally regulated during normal liver development. Gastroenterology 2004;126:1134-1146.
9) Apte U, Zeng G, Thompson MD, Muller P, Micsenyi A, Cieply B, et al. Beta-catenin is critical for early postnatal liver growth. Am J Physiol Gastrointest Liver Physiol 2007;292:G1578-G1585.
10) Thompson MD, Monga SPS. WNT/β-catenin signaling in liver health and disease. Hepatology 2007;45:1298-1305.
11) Tan X, Yuan Y, Zeng G, Apte U, Thompson MD, Cieply B, et al. Beta-catenin deletion in hepatoblasts disrupts hepatic morphogenesis and survival during mouse development. Hepatology 2008;47:1667-1679.
12) Wang B, Zhao L, Fish M, Logan CY, Nusse R. Self-renewing diploid Axin2$^+$ cells fuel homeostatic renewal of the liver. Nature 2015;524:180-185.
13) Yang J, Mowry LE, Nejak-Bowen KN, Okabe H, Diegel CR, Lang RA, et al. Beta-catenin signaling in murine liver zonation and regeneration: a Wnt-Wnt situation! Hepatology 2014;60:964-976.
14) Sekine S, Gutiérrez PJA, Yu-Ang Lan B, Feng S, Hebrok M. Liver-specific loss of β-catenin results in delayed hepatocyte proliferation after partial hepatectomy. Hepatology 2007;45:361-368.
15) Nejak-Bowen KN, Thompson MD, Singh S, Bowen WC, Dar MJ, Khillan J, et al. Accelerated liver regeneration and hepatocarcinogenesis in mice overexpressing serine-45 mutant beta-catenin. Hepatology 2010;51:1603-1613.
16) Ding B-S, Nolan DJ, Butler JM, James D, Babazadeh AO, Rosenwaks Z, et al. Inductive angiocrine signals from sinusoidal endothelium are required for liver regeneration. Nature 2010;468:310-315.
17) **Planas-Paz L**, **Orsini V**, Boulter L, Calabrese D, Pikiolek M, Nigsch F, et al. The RSPO-LGR4/5-ZNRF3/RNF43 module controls liver zonation and size. Nat Cell Biol 2016;18:467-479.
18) Rocha AS, Vidal V, Mertz M, Kendall TJ, Charlet A, Okamoto H, et al. The angiocrine factor Rspondin3 is a key determinant of liver zonation. Cell Rep 2015;13:1757-1764.
19) Lustig B, Jerchow B, Sachs M, Weiler S, Pietsch T, Karsten U, et al. Negative feedback loop of Wnt signaling through upregulation of conductin/Axin2 in colorectal and liver tumors. Mol Cell Biol 2002;22:1184-1193.
20) van Amerongen R, Bowman AN, Nusse R. Developmental stage and time dictate the fate of Wnt/β-catenin-responsive stem cells in the mammary gland. Cell Stem Cell 2012;11:387-400.
21) Madisen L, Zwingman TA, Sunkin SM, Oh SW, Zariwala HA, Gu H, et al. A robust and high-throughput Cre reporting and characterization system for the whole mouse brain. Nat Neurosci 2010;13:133-140.
22) Brault V, Moore R, Kutsch S, Ishibashi M, Rowitch DH, McMahon AP, et al. Inactivation of the beta-catenin gene by Wnt1-Cre-mediated deletion results in dramatic brain malformation and failure of craniofacial development. Development 2001;128:1253-1264.
23) Carpenter AC, Rao S, Wells JM, Campbell K, Lang RA. Generation of mice with a conditional null allele for Wntless. Genesis 2010;48:554-558.
24) Schwenk F, Baron U, Rajewsky K. A cre-transgenic mouse strain for the ubiquitous deletion of loxP-flanked gene segments including deletion in germ cells. Nucleic Acids Res 1995;23:5080.
25) **Wang Y**, **Nakayama M**, **Pitulescu ME**, **Schmidt TS**, Bochenek ML, Sakakibara A, et al. Ephrin-B2 controls VEGF-induced angiogenesis and lymphangiogenesis. Nature 2010;465:483-486.
26) Livak KJ, Schmittgen TD. Analysis of relative gene expression data using real-time quantitative PCR and the 2(-Delta Delta C(T)) method. Methods 2001;25:402-408.
27) Tabula Muris Consortium. Single-cell transcriptomics of 20 mouse organs creates a Tabula Muris. Nature 2018;562:367-372.
28) Ghafoory S, Breitkopf-Heinlein K, Li Q, Scholl C, Dooley S, Wölfl S. Zonation of nitrogen and glucose metabolism gene expression upon acute liver damage in mouse. PLoS One 2013;8:e78262.
29) Jho E-H, Zhang T, Domon C, Joo C-K, Freund J-N, Costantini F. Wnt/beta-catenin/Tcf signaling induces the transcription of Axin2, a negative regulator of the signaling pathway. Mol Cell Biol 2002;22:1172-1183.
30) **Ding B-S**, **Cao Z**, Lis R, Nolan DJ, Guo P, Simons M, et al. Divergent angiocrine signals from vascular niche balance liver regeneration and fibrosis. Nature 2014;505:97-102.
31) Bhathal PS, Rose NR, Mackay IR, Whittingham S. Strain differences in mice in carbon tetrachloride–induced liver injury. Br J Exp Pathol 1983;64:524-533.
32) Relaix F, Zammit PS. Satellite cells are essential for skeletal muscle regeneration: the cell on the edge returns centre stage. Development 2012;139:2845-2856.
33) Gregorieff A, Liu Y, Inanlou MR, Khomchuk Y, Wrana JL. Yap-dependent reprogramming of Lgr5$^+$ stem cells drives intestinal regeneration and cancer. Nature 2015;526:715-718.
34) Barker N, Van Es JH, Kuipers J, Kujala P, van den Born M, Cozijnsen M, et al. Identification of stem cells in small intestine and colon by marker gene Lgr5. Nature 2007;449:1003-1007.
35) Yan KS, Chia LA, Li X, Ootani A, Su J, Lee JY, et al. The intestinal stem cell markers Bmi1 and Lgr5 identify two functionally distinct populations. Proc Natl Acad Sci USA 2012;109:466-471.
36) **Halpern KB**, **Shenhav R**, Massalha H, Tóth B, Egozi A, Massasa EE, et al. Paired-cell sequencing enables spatial gene expression mapping of liver endothelial cells. Nat Biotechnol 2018;5:279-215.
37) **Hu J**, **Srivastava K**, Wieland M, Runge A, Mogler C, Besemefelder E, et al. Endothelial cell–derived angiopoietin-2 controls liver regeneration as a spatiotemporal rheostat. Science 2014;343:416-419.
38) Manavski Y, Abel T, Hu J, Kleinlützum D, Buchholz CJ, Belz C, et al. Endothelial transcription factor KLF2 negatively regulates liver regeneration via induction of activin A. Proc Natl Acad Sci USA 2017;114:3993-3998.
39) Gomez-Salinero JM, Rafii S. Endothelial cell adaptation in regeneration. Science 2018;362:1116-1117.
40) Tan X, Behari J, Cieply B, Michalopoulos GK, Monga SPS. Conditional deletion of β-catenin reveals its role in liver growth and regeneration. Gastroenterology 2006;131:1561-1572.

Author names in bold designate shared co-first authorship.

Supporting Information

Additional Supporting Information may be found at onlinelibrary.wiley.com/doi/10.1002/hep.30563/suppinfo.